Mutation of αPhe55 of Methylamine Dehydrogenase Alters the Reorganization Energy and Electronic Coupling for Its Electron Transfer Reaction with Amicyanin[†,‡]

Dapeng Sun,[§] Zhi-wei Chen,[||] F. Scott Mathews,[||] and Victor L. Davidson*[,§]

Department of Biochemistry, The University of Mississippi Medical Center, Jackson, Mississippi 39216-4505, and Department of Biochemistry and Molecular Biophysics, Washington University School of Medicine, St. Louis, Missouri 63110

Received August 15, 2002; Revised Manuscript Received September 18, 2002

ABSTRACT: Methylamine dehydrogenase (MADH) possesses an $\alpha_2\beta_2$ structure with each smaller β subunit possessing a tryptophan tryptophylquinone (TTQ) prosthetic group. Phe55 of the α subunit is located where the substrate channel from the enzyme surface opens into the active site. Site-directed mutagenesis of αPhe55 has revealed roles for this residue in determining substrate specificity and binding monovalent cations at the active site. It is now shown that the αF55A mutation also increases the rate of the true electron transfer (ET) reaction from O-quinol MADH to amicyanin. The reorganization energy associated with the ET reaction is decreased from 2.3 to 1.8 eV. The electronic coupling associated with the ET reaction is decreased from 12 to 3 cm^{-1}. The crystal structure of αF55A MADH in complex with its electron acceptors, amicyanin and cytochrome *c*-551i, has been determined. Little difference in the overall structure is seen, relative to the native complex; however, there are significant changes in the solvent content of the active site and substrate channel. The crystal structure of αF55A MADH has also been determined with phenylhydrazine covalently bound to TTQ in the active site. Phenylhydrazine binding significantly perturbs the orientation of the TTQ rings relative to each other. The ET results are discussed in the context of the new and old crystal structures of the native and mutant enzymes.

Methylamine dehydrogenase (MADH)[1] from *Paracoccus denitrificans* is a tryptophan tryptophylquinone (TTQ) dependent enzyme that catalyzes the oxidative deamination of methylamine to formaldehyde and ammonia and the subsequent electron transfer (ET) to a type I copper protein, amicyanin (eqs 1 and 2) (*1*). The structure of MADH is that

$$CH_3NH_3^+ + TTQ_{ox} + H_2O \rightarrow HCHO + TTQ_{red}\text{-}NH_2 + H^+ \quad (1)$$

$$TTQ_{red}\text{-}NH_2 + 2amicyanin_{ox} \rightarrow 2amicyanin_{red} + TTQ_{ox} + NH_4^+ + H^+ \quad (2)$$

of an $\alpha_2\beta_2$ heterotetramer (*2*). Each β subunit possesses a TTQ prosthetic group (*3*) that is formed by posttranslational modifications of Trp57 and Trp108 of the β subunit (*2*) (Figure 1). MADH and amicyanin form one of the best characterized physiologic ET complexes of proteins. Crystal structures are available for the binary complex of MADH and amicyanin (*4*) and for a ternary protein complex (*5*) which also includes cytochrome *c*-551i, which is the electron acceptor for amicyanin. The spectroscopic properties of the different redox forms of these proteins have been characterized (*6*).

Stopped-flow spectroscopy has been applied to study the ET reactions between different redox forms of TTQ and the type I copper center of amicyanin (*7*−*10*). Analysis of the ET reactions from substrate-reduced MADH (N-quinol MADH) to amicyanin (*7*, *8*) indicates that this ET is gated by a preceding proton transfer step (Figure 2). The observed rate constant (k_{obs}) that is measured is actually not the true ET rate constant (k_{ET}) but the rate of the preceding proton transfer. By titration with dithionite, O-quinol and O-semiquinone forms of MADH can be generated (*6*). In contrast to the gated reaction of the N-quinol MADH, the reaction of the O-quinol MADH with amicyanin is a true ET reaction with $k_{obs} = k_{ET}$ (*9*, *10*). The temperature and $\Delta G°$ dependencies of the rates of the ET reactions between O-forms of MADH and amicyanin were determined (*9*, *10*) and analyzed by ET theory (*11*) to obtain values for the reorganization energy (λ) and electronic coupling (H_{AB}) that are associated with these reactions. The ET distance which was also obtained from these analyses (*9*) closely

[†] This work was supported by NIH Grant GM-41574 (V.L.D.) and NSF Grant MCB-00091084 (F.S.M.).

[‡] Crystallographic coordinates have been deposited in the Protein Data Bank under the file names 1GM2 (αF55A MADH−amicyanin−cytochrome *c*-551i complex) and 1GM3 (phenylhydrazine adduct of the complex).

* Corresponding author. Telephone: 601-984-1516. Fax: 601-984-1501. E-mail: vdavidson@biochem.umsmed.edu.

[§] The University of Mississippi Medical Center.

[||] Washington University School of Medicine.

[1] Abbreviations: MADH, methylamine dehydrogenase; TTQ, tryptophan tryptophylquinone; ET, electron transfer; H_{AB}, electronic coupling; λ, reorganizational energy; AADH, aromatic amine dehydrogenase; O-quinol, fully reduced TTQ with oxygen at the C6 carbon; N-quinol, fully reduced TTQ with nitrogen bonded to the C6 carbon; MR, molecular replacement; NCS, noncrystallographic symmetry; Trq, the quinolated tryptophan residue; E_m, oxidation−reduction midpoint potential.

10.1021/bi026654x CCC: $22.00
Published on Web 10/30/2002

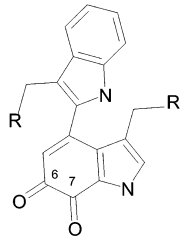

FIGURE 1: Structure of tryptophan tryptophylquinone (TTQ). The C6 and C7 carbonyl carbons are labeled. R indicates connections to the polypeptide chain.

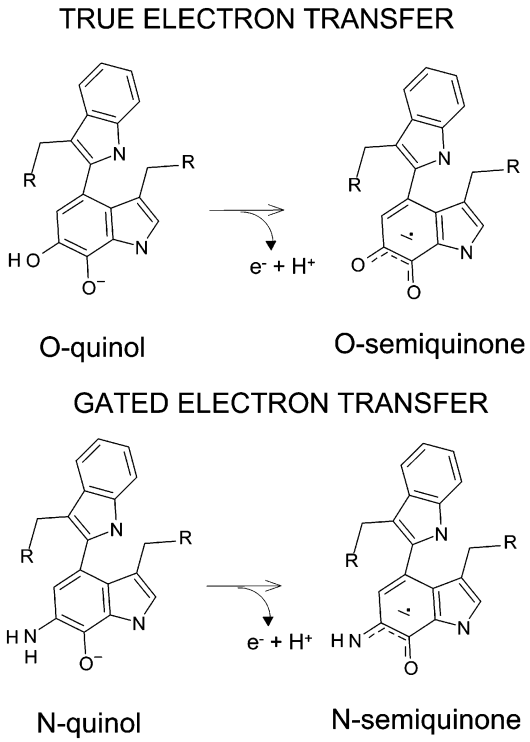

FIGURE 2: Electron transfer reactions from different forms of reduced TTQ in methylamine dehydrogenase. The ET reactions from these two redox forms of MADH follow different kinetic mechanisms. For the N-quinol, deprotonation precedes ET and is slower than ET. Therefore, the reaction is gated, and the observed rate is a proton transfer rate. For the O-quinol, the ET is rate limiting for the overall reaction so this is a true electron transfer reaction, and the observed rate is k_{ET}. In these reactions the electron acceptor is amicyanin.

matched the distance between the redox centers which is seen in the crystal structure of the protein complexes.

The ET reaction from O-quinol MADH to amicyanin exhibits a relatively large λ value of about 2.3 eV (*9*, *10*). The kinetic or structural basis for this large λ value is not known. If this were really not a true ET reaction but, instead, a conformationally coupled ET reaction, then the large λ could arise from kinetic complexity. In such a case, a structural rearrangement of the MADH−amicyanin complex would be required for the achievement of the optimum orientation for ET. If that rearrangement were faster than the ET rate but energetically unfavorable (i.e., $K_{eq} \ll 1$), then k_{obs} would be an apparent k_{ET} equal to the product of K_{eq} for the non-ET reaction step and the true ET rate constant (i.e., $k_{obs} = K_{eq}k_{ET}$) (*12*, *13*). The λ value obtained from the analysis of the temperature dependence of the rate of a coupled ET reaction will contain contributions from K_{eq} as well as k_{ET} (*14*). It is often difficult to distinguish between true and coupled ET reactions solely on the basis of temperature dependence studies. In the case of the reaction between O-quinol MADH and amicyanin, it was proven that this is a true ET reaction by demonstrating that the same λ value was obtained from both temperature and $\Delta G°$ dependence studies of the reaction rate (*10*). This would not be expected for a coupled ET reaction (*14*). Furthermore, mutations at the MADH−amicyanin interface that affected binding had no effect on the λ for the ET reaction from TTQ to copper (*15*). Thus, the large λ for this reaction is not believed to be due to kinetic complexity.

If the large λ does not arise from kinetic complexity, then it must arise from reorganization of the redox centers, protein matrix, and solvent. The inner sphere λ for type I copper centers is relatively low (<1 eV) (*16*). The λ value for the ET reaction of reduced amicyanin with its electron acceptor cytochrome *c*-551i is 1.1 eV (*17*). This suggests that the large λ for the reaction of amicyanin with MADH is due primarily to contributions from MADH and TTQ.

In this paper we describe a site-directed mutation of MADH which significantly lowers the λ for the ET reaction of O-quinol MADH with amicyanin. Residue Phe55 of the noncatalytic α subunit has been converted to Ala by site-directed mutagenesis (*18*). αPhe55 is located at the interface between the α and β subunits and forms a part of the substrate channel which connects the active site to the enzyme surface. The αF55A MADH has similar spectral properties but a different substrate specificity from the native MADH (*18*). The αF55A mutation also influences monovalent cation binding at the active site of MADH (*19*). It increases the K_d value associated with cation-dependent spectral perturbations of MADH. It also decreases the K_d value associated with monovalent cation stimulation of gated ET from N-quinol MADH to amicyanin (*19*). In this paper, we show that the rate of the true ET reaction from the O-quinol αF55A MADH to amicyanin is much faster than that of native MADH. This is due to a 0.5 eV decrease in λ that is caused by the αF55A mutation. The X-ray crystal structures of the ternary complexes of αF55A MADH and αF55A MADH with phenylhydrazine bound to TTQ are also presented. The ET results are discussed in the context of these new structures.

EXPERIMENTAL PROCEDURES

Materials. Native MADH was purified from *P. denitrificans* as described previously (*20*). The αF55A MADH was heterologously expressed in *Rhodobacter sphaeroides* (*21*) and purified as described previously (*18*). O-Quinol MADH was generated by anaerobic titration of oxidized MADH with stoichiometric amounts of sodium dithionite. N-Quinol MADH was generated by titration of oxidized MADH with stoichiometric amounts of methylamine. All reagents were purchased from commercial sources and used without further purification.

Biochemical Measurements. Transient kinetic experiments were performed using an On-Line Instrument Systems (OLIS) RSM16 stopped-flow spectrophotometer. The reactions were performed in 10 mM potassium phosphate buffer, pH 7.5, at the indicated temperature. MADH was the limiting reactant with its concentration fixed at 2 μM. Pseudo-first-

order conditions were maintained so that the concentration of amicyanin was much greater than that of MADH and well above the K_d for complex formation at each temperature. Reactions were monitored between 320 and 560 nm. Kinetic data collected in the rapid-scanning mode were reduced by factor analysis using the singular value decomposition algorithm and then globally fit by the Levenberg and Marquardt nonlinear method of least squares using the fitting routines of the OLIS Global Fit software. Details of the method of data analysis have been previously described (*8*). The oxidation−reduction midpoint potential (E_m) value of αF55A MADH was determined by spectrochemical titration as previously described (*22*).

Crystallization and Data Collection. Crystals of the αF55A mutant ternary complex were grown by the sitting drop method as described previously (*23*). Equal volumes of 5 μL each of protein solution (9.6 mg/mL αF55A MADH, 2.9 mg/mL amicyanin, 4.8 mg/mL cytochrome *c*-551i in 5 mM Na^+/K^+ phosphate buffer, pH 5.0) and reservoir solution [2.4 M Na^+/K^+ monobasic/dibasic phosphate buffer (80%:20% by volume), pH ~5.0] were mixed and allowed to equilibrate. It should be noted that MADH retains activity in solution at this pH (*24*) and that MADH activity in the crystalline state has been demonstrated at pH 5.7 (*25*).

X-ray data were recorded from single crystals at 100 K on a Rigaku R-axis II image plate detector using a graphite monochromatized X-ray beam obtained from a Rigaku RU200 X-ray generator operated at 5 keV power. The crystals were soaked with 20% glycerol as a cryoprotectant added to an artificial mother liquor (2.4 M Na^+/K^+ phosphate, 80%:20%) in 5% increments over a 15 min period and flash frozen at 100 K. The phenylhydrazine derivative was obtained by soaking a mutant ternary crystal in artificial mother liquor saturated with phenylhydrazine for 30 min prior to freezing. The crystals were monoclinic, space group $P2_1$, with unit cell parameters $a = 79.12$ Å, $b = 188.20$ Å, $c = 127.10$ Å, and $\beta = 99.24°$ for the ligand free complex and $a = 79.52$ Å, $b = 188.37$ Å, $c = 127.37$ Å, and $\beta = 98.84°$ for the phenylhydrazine derivative. There are two heterooctameric molecules ($2 \times \alpha_2\beta_2AMI_2CYT_2$) per asymmetric unit. Spot integration and data scaling were carried out using HKL (*26*). The data were generally 81−87% complete overall and scaled to the outer resolution limits (2.25−2.40 Å) with R_{merge} between 0.074 and 0.093. The data collection statistics are summarized in Table 1.

Refinement of the Structures. The initial coordinates of the αF55A MADH mutant ternary complex were obtained by molecular replacement (MR) with AMORE (*27*) using the wild-type ternary complex (*5*) with all waters omitted as a search model. The phenylhydrazine-bound mutant complex was refined directly from the mutant complex structure. Extra electron density in the active site was fitted with a phenylhydrazine model obtained from the Cambridge Structure Database (*28*). The refinement and electron density map calculations were carried out using CNS (*29*), and 10% of the reflections were selected randomly and set aside as a test set for cross-validation (*30*). Reflections from 30 to 2.25 or 2.40 Å resolution for each data set were included in the refinements, although those with $\sigma(I) < 0.0$ were omitted; a bulk solvent correction was applied (*31*). Noncrystallographic symmetry (NCS) restraints were applied to the four α and β subunits of MADH in the asymmetric unit during refinement with NCS weights set to 300 for both main and side chain atoms. No NCS restraints were applied to the amicyanin or cytochrome components. The differences between *B*-factors for bonded atoms were restrained with target standard deviations of 1.5 Å^2 for main chain and 2.0 Å^2 for side chain atoms. Model building and analysis of the structures were carried out on a Silicon Graphics workstation using Turbo-Frodo (*32*). Several cycles of positional and temperature factor refinement, followed by interactive model building and automatic solvent placement with manual examination, were carried out. This procedure utilized electron density difference maps calculated with Fourier coefficients ($2F_o - F_c$) and ($F_o - F_c$), where F_o and F_c are the observed and calculated structure factors, respectively.

Table 1: Data Collection and Structure Determination Statistics of αF55A MADH−Amicyanin−Cytochrome *c*-551i Ternary Complexes[a]

crystal	αF55A MADH complex	αF55A MADH−phenylhydrazine complex
data collection		
temperature (K)	100	100
resolution (Å)	50.0−2.25	50.0−2.4
no. of reflections	150718	117875
completeness (all/outer 0.05 Å shell, %)	87.0/47.4	81.3/50.7
R_{merge}[a] (all/outer)	0.074/0.201	0.093/0.246
$\langle I\rangle/\sigma$[b] (all/outer)	15.7/4.0	9.3/2.2
redundancy (all/outer 0.05 Å shell)	4.5/2.1	3.7/2.0
refinement		
R_{cryst}[c] (all/outer 0.05 Å shell)	0.173/0.222	0.193/0.377
R_{free}[d] (all/outer 0.05 Å shell)	0.210/0.278	0.246/0.397
no. of protein atoms (non-H)	23476	23508
$\langle B\rangle$ (Å^2)	22.7	30.8
no. of copper	4	4
$\langle B\rangle$ (Å^2)	23.3	41.4
no. of heme groups	4	4
$\langle B\rangle$ (Å^2)	19.7	30.4
no. of sodium ions	4	4
$\langle B\rangle$ (Å^2)	14.9	24.2
no. of PO_4^{3-} groups	8	8
$\langle B\rangle$ (Å^2)	67.5	84.7
no. of solvent molecules	1685	842
$\langle B\rangle$ (Å^2)	23.7	23.1
RMSD bonds (Å)	0.006	0.006
RMSD angles (deg)	1.41	1.42
RMSΔB (main−main, Å^2)	1.8	2.6
RMSΔB (main−side, Å^2)	2.3	3.3
RMSΔB (side−side, Å^2)	3.2	4.2

[a] $R_{merge} = \sum_h\sum_i|I(h) - I_i(h)|/\sum_h\sum_i I_i(h)$, where $I_i(h)$ and $I(h)$ are the *i*th and mean measurements of reflection *h*. [b] $I/\sigma(I)$ is the average signal to noise ratio for merged reflection intensities. [c] $R = \sum_h|F_o - F_c|/\sum_h|F_o|$, where F_o and F_c are the observed and calculated structure factor amplitudes of reflection *h*. [d] R_{free} is the test reflection data set, about 10% selected randomly for cross-validation during crystallographic refinement.

The quality of the refined structures and the resulting electron density maps of both structures are high (Table 1, Figures 3 and 4). *R* and R_{free} range from 0.173 to 0.193 and 0.210 to 0.246, respectively, with RMSD in bond length and angles of 0.006 Å and 1.41−1.42°, respectively. In addition to the four TTQ, heme, and copper prosthetic groups, four sodium ions and eight phosphate groups were located in each crystal. In addition, between 842 and 1685 water molecules are included in the structures. The Ramachandran plot (*33*, *34*) for each crystal structure shows that 11 residues per

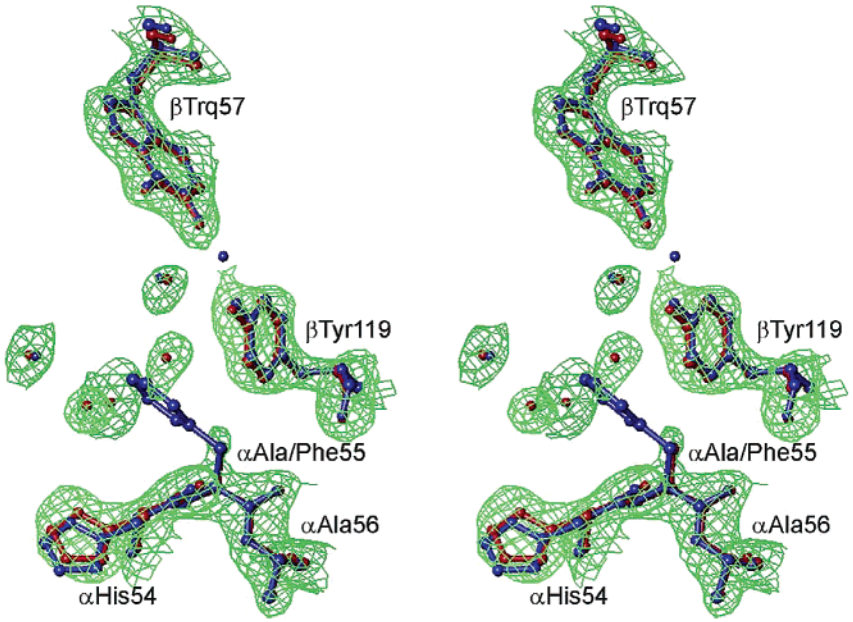

FIGURE 3: Electron density of the αF55A mutant ternary complex computed using coefficients ($2F_o - F_c$) and contoured at 1.25σ. Shown in red is the refined model of the mutant complex for selected residues (αHis54−αAla56, βTrq57, βTyr119), several waters leading into the active site, and one water within the active site. The superimposed model of wild-type MADH with two water molecules inside the active site and one outside is shown in blue.

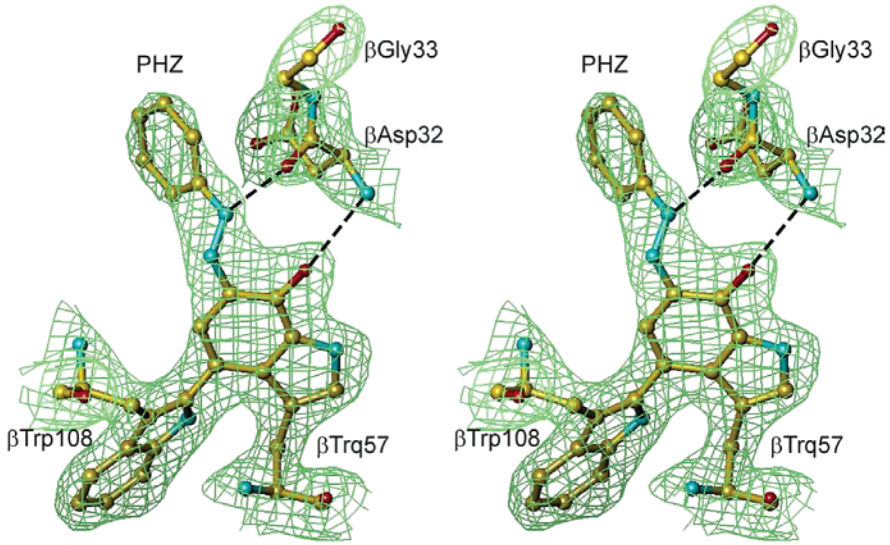

FIGURE 4: Electron density of the αF55A mutant ternary complex after the crystal was soaked with phenylhydrazine computed using coefficients ($2F_o - F_c$) and contoured at 1.5σ. The TTQ cofactor with phenylhydrazine attached along with residue βAsp32 to which TTQ and phenylhydrazine each form a hydrogen bond is also shown, along with the adjacent βGly33.

asymmetric unit lie in a sterically disallowed region. The final refinement statistics are shown in Table 1.

RESULTS

General Structural Features. Both the αF55A MADH ternary complex and its phenylhydrazine adduct crystallize in a monoclinic unit cell containing two heterooctamers, or 16 protomers, in the asymmetric unit. This differs from the originally published ternary complex that crystallized in a C-centered orthorhombic cell and contained one heterotetramer, or four protomers, in the asymmetric unit (*23*). It is, however, consistent with subsequent crystallization experiments with the wild-type ternary complex that all yield the monoclinic form below pH 7 (unpublished results). The reason for the change in space group is not apparent.

The 11 sterically disallowed residues of the αF55A mutant ternary complex occur at three positions in the four heterotetramers. Two correspond to tightly packed interior residues of the α subunit that are also found in the same conformation in the uncomplexed native MADH structure determined at 1.75 Å resolution (2) and in the structure of MADH from *Methylobacterium extorquens* AM1 (*35*). The third is located in three of the cytochrome subunits very close to a "generously allowed" region.

Structural Features of α*F55A MADH.* The αF55A MADH portion of the mutant ternary complex is very similar in conformation to that of wild-type uncomplexed MADH (*2*) with an RMS deviation between them of 0.38 Å for equivalent Cα atoms. However, the αF55A MADH contains 27 additional residues at the N-terminal end of the α subunit

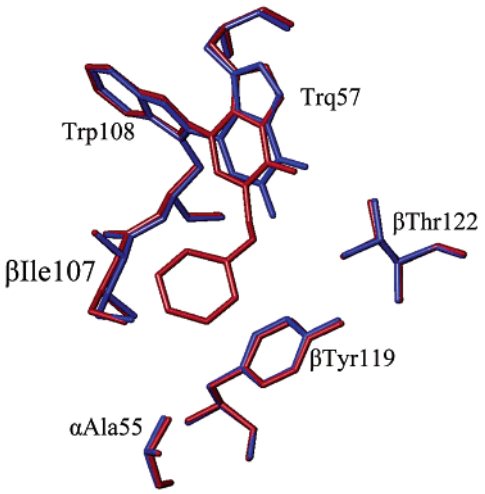

FIGURE 5: Effect of phenylhydrazine binding on TTQ in αF55A MADH. The refined models for selected residues of αF55A MADH (blue) and αF55A MADH after being soaked in phenylhydrazine (red) are superimposed.

that had been cleaved by proteolysis in the native crystals. This extended tail forms a helix−turn motif that folds over the β subunit of the second $\alpha\beta$ heterodimer as observed in the crystal structure of MADH from *M. extorquens* AM1 (*35*).

The only significant differences between native and mutant MADH within the active site pocket are the replacement of αPhe55 by Ala and a slight movement of the αHis54 residue (Figure 3). In wild-type MADH the pocket is lined by main chain and side chain residues all located in the β subunit with the exception of αPhe55, located at the opposite end of the pocket from TTQ. This side chain blocks bulk solvent access to the pocket through a channel between the α and β subunits (*2*). In the wild-type enzyme the cavity contains two weakly occupied solvent molecules with thermal *B* values ∼45 Å^2. In the αF55A MADH ternary complex, αPhe55 is replaced by Ala. Only one of these native "inner" waters is retained and generally a second or third water ("outer") occupies space normally occupied by αPhe55. These waters are somewhat better ordered ($B = 25-30$ Å^2) than in the native. The inner waters form hydrogen bonds to main or side chain oxygen atoms, but the outer waters tend to make hydrogen bonds only to the inner water and to each other and less so to bulk solvent molecules beyond αAla55.

Phenylhydrazine Binding to αF55A MADH. In the αF55A MADH mutant ternary complex crystals soaked in the presence of phenylhydrazine, the ligand is bound to C6 of TTQ, replacing O6 in all four active sites in the asymmetric unit (Figure 4). Previous attempts to locate a bound ligand in crystals of phenylhydrazine-inhibited MADH from *P. denitrificans* have failed (unpublished results), presumably because of the small size of the active site pocket. It was expected that removal of the bulky phenyl ring from position α55 would permit the equally bulky inhibitor to bind to the crystalline enzyme, as borne out by the results.

Binding of phenylhydrazine to the αF55A MADH causes only minimal structural changes to occur (Figure 5). The water molecules in the active site are displaced by the phenyl ring of phenylhydrazine, and N1 of the latter forms a hydrogen bond to the carbonyl oxygen of βAsp32. As a result, the quinolated Trp (Trq) ring of TTQ is tilted by about 10°, the βAsp32O atom moves by about 0.7 Å, and the associated backbone moves by about 0.4 Å. Other backbone displacements of 0.2−0.3 Å occur elsewhere in the active site and in the remainder of the molecule and probably represent random fluctuations or errors in the coordinates.

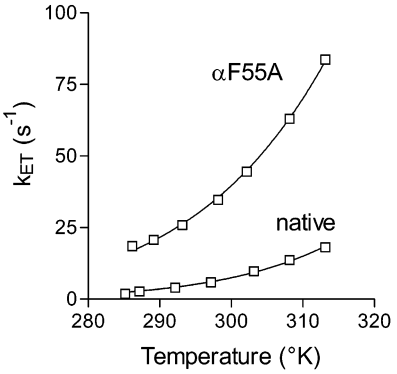

FIGURE 6: Effect of the αF55A mutation on the true electron transfer reaction from O-quinol methylamine dehydrogenase to oxidized amicyanin. Solid lines represent fits of the data to eq 3.

The studies of the αF55A mutant of MADH confirm that no global structural changes in the molecule occur other than the local exchange of a phenyl ring by a methyl group. This mutation enables the binding of the bulky phenylhydrazine to N6 of TTQ to be observed for the first time in MADH as a result of the enlargement of the active site pocket.

Temperature Dependence and Marcus Analysis of ET Rate. Measurement of the ET rate constant (k_{ET}) for the reaction of the O-quinol form of αF55A MADH with amicyanin was performed at different temperatures ranging from 12 to 40 °C. The k_{ET} for the reaction of αF55A MADH is about 4−10-fold faster than that of the native MADH, depending upon the temperature (Figure 6). The variation with temperature of these limiting first-order rate constants for the ET reaction were analyzed by ET theory (eq 3), where

$$k_{ET} = \frac{4\pi^2 H_{AB}{}^2}{h\sqrt{4\pi\lambda RT}} e^{-(\Delta G^\circ + \lambda)^2/4\lambda RT} \quad (3)$$

λ is the reorganization energy, H_{AB} is the electronic coupling matrix element, h is Planck's constant, T is temperature, and R is the gas constant.

The E_m value for the quinone/quinol redox couple of αF55A MADH was determined by spectrochemical titration and found to be essentially the same as that of native MADH (data not shown). Thus, the same ΔE_m value of −31 mV was used to determine ΔG° in eq 3 for the reactions with amicyanin of either native or αF55A MADH. This value was previously shown by kinetic analysis to be the driving force for the one-electron oxidation by amicyanin of O-quinol MADH to the O-semiquinone (*10*). Values of λ and H_{AB} for the reactions of αF55A MADH were obtained by fitting the data shown in Figure 6 to eq 3. Both of the values of λ and H_{AB} for the reactions of αF55A MADH are smaller than those of native MADH. The value of λ for the reactions of αF55A MADH is 1.8 ± 0.1 eV compared to 2.3 ± 0.1 eV for native MADH. If all other parameters were unchanged, then the 0.5 eV decrease in λ will cause the ET rate to increase by approximately 60−160-fold depending on the temperature. However, the value of H_{AB} for the reactions of

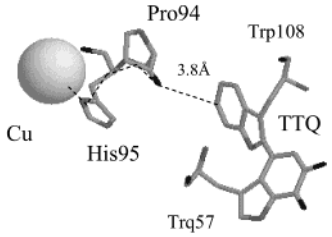

FIGURE 7: Predicted pathway for interprotein electron transfer from TTQ to copper. Results of a Pathways analysis of the relevant portion of the crystal structure of the complex with native MADH are shown. The pathway from TTQ to copper involves a through-space jump (dashed line) from the surface-exposed Trp108 indole ring of TTQ to the carbonyl O of Pro94 of amicyanin, followed by passage through six covalent bonds (solid line) via the His95 ligand to copper.

αF55A MADH is 3.0 ± 1.2 cm^{-1} compared to 12 ± 7 cm^{-1} for native MADH. The 4-fold decrease in H_{AB} will cause the ET rate to decrease by 16-fold (see eq 3). Thus, the observed 4−10-fold increase in ET rate is determined by the combination of the changes in λ and H_{AB}.

DISCUSSION

As can be seen in eq 3, the activation energy for an ET reaction is $(\Delta G^\circ + \lambda)^2/4\lambda$. H_{AB} determines the efficiency of the ET after achievement of the transition state. Comparison of the λ and H_{AB} values for the reactions of αF55A MADH and native MADH indicates that, during ET, αF55A MADH needs to overcome a smaller activation energy barrier than that of native MADH (i.e., a smaller λ) and that, after the achievement of the transition state, the αF55A MADH has a lower efficiency of ET to amicyanin than that of native MADH (i.e., a smaller H_{AB}).

Correlation of Changes in λ with Structure. Residue αPhe55 is located approximately 7 Å from TTQ and is not on the predicted pathway for ET to copper (Figure 7). Comparison of the structures of the active sites of native and αF55A MADH shows no significant differences in structure, other than the removal of the phenyl ring from the side chain of residue α55 (Figure 3). This provides no clear basis for the 0.5 eV reduction in the λ for the reaction of αF55A MADH. Two possible explanations are discussed below. One involves reorientation of the TTQ rings in concert with ET. The other involves differences in solvent reorganization.

It is possible that the orientation of the TTQ rings with respect to each other changes during the ET reaction. Although the oxidized and reduced structures of native and αF55A MADH are very similar (unpublished results), the phenylhydrazine-bound αF55A MADH structure reveals a significant change in the dihedral angle between TTQ rings. If reorientation of the TTQ rings occurs in concert with ET, then this would contribute to λ. If this movement is less restricted in αF55A MADH, then a decrease in λ would be observed.

It is surprising that the mutation of a residue in the α subunit affects the λ of the TTQ cofactor in the β subunit. This interaction may be mediated by interactions with residue βIle107. From Figure 8, it is observed that the phenyl ring of the αPhe55 residue is in close contact with the side chain of the βIle107 in the β subunit. The importance of this interaction was proven in previous work (*36*), in which

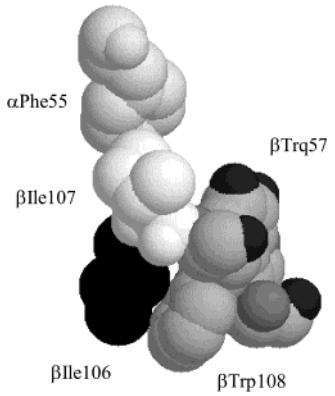

FIGURE 8: Positions of βIle106 and βIle107 relative to αPhe55 and TTQ. These residues are drawn as space-filling models to indicate potential interactions.

βIle107 was changed to Val and Asn. Although βIle107 is positioned behind αPhe55 relative to the substrate channel, βI107V and βI107N mutations altered the substrate specificity of MADH by altering the position of αPhe55 (*36*). It follows that removal of the phenyl ring of αPhe55 will allow the side chain of βIle107 increased freedom of motion. This movement will likely cause perturbations in the positions of the side chains of the adjacent residues, βTrp108 and βIle106, through changes in the orientation and the position of the βIle107 backbone. Residue βTrp108, of course, is a component of TTQ. The βIle106 side chain also makes close contact with the indole ring of βTrp108 and may influence its freedom of movement. Thus, allowing more freedom of motion of βIle107 may facilitate reorientation of the βTrp108 moiety of TTQ relative to the βTrp57 ring of TTQ during ET. It is clear from the phenylhydrazine-bound structure of αF55A MADH that movement of TTQ rings relative to each other can occur (Figure 5). Interaction between TTQ and αPhe55 was also indicated in studies of the mechanism-based inactivation of MADH by cyclopropylamine (*37*). This inactivation results in covalent cross-linking of the α and β subunits of MADH. While the identity of the amino acid residue involved in the cross-link could not be determined, αF55A and αF55I MADH do not undergo such cross-linking (*37*), suggesting that the cross-link involves αPhe55 and TTQ. Since the distance that separates the two is too long to be bridged by the three-carbon cross-linker derived from cyclopropylamine, it seems likely that movement of αPhe55 and TTQ relative to each other occurs during the reaction cycle.

Correlation of Changes in λ with Solvent Reorganization in the Active Site. λ is comprised of λ_{in} and λ_{out}, and the reorganization of water molecules can contribute substantially to λ_{out}. Two water molecules are present in the native MADH active site at a distance shorter than 5 Å from TTQ and shielded from the bulk solvent by αPhe55. Only one water within close proximity to TTQ is seen in the αF55A MADH active site (Figure 3). Additional waters are present in the αF55A MADH structure in the space created by the removal of the phenyl ring, but these reside further from TTQ and do not appear to participate in H-bonding interactions with TTQ or active site residues. If the reorganization of solvent contributes to the λ for ET from MADH, then the reorganization of the inner waters in close proximity to TTQ would be significant. If TTQ is less solvated in αF55A MADH (Figure 3), then this would be expected to decrease λ by

decreasing λ_{out}. Inspection of structures of several different crystals of MADH reveals some variability in the numbers of water molecules in the active site (data not shown). Thus, it is difficult to define precisely how the waters are distributed in the active sites. It is noteworthy that previous studies showed that αF55A MADH prefers long-chain amines over methylamine (*18*). The optimum substrate is a seven-carbon chain amine. This suggests that the mutant has a more hydrophobic active site, despite creating a more open access to the substrate channel and bulk solvent. It is also worth noting the results of similar ET studies with the TTQ−enzyme aromatic amine dehydrogenase (AADH) and its electron acceptor, azurin (*38*). Analysis of the ET reaction of AADH with azurin yielded a value of $\lambda = 1.6$ eV (*38*), similar to that observed for αF55A MADH and amicyanin. The structure of AADH is not known, but on the basis of sequence comparison these proteins are very similar to the MADH−amicyanin system. The sequence identity between AADH and MADH is 60% for the β subunits and 31% for the α subunits (*39*). The active site residues of the β subunit of AADH are conserved in MADH. AADH prefers phenylethylamines as substrates, and structure−reactivity studies showed that the active site of AADH prefers hydrophobic substrates (*40*), consistent with a decreased water content in the active site of AADH and consistent with it exhibiting a λ value more similar to that exhibited by αF55A MADH than native MADH.

Correlation of Changes in H_{AB} with Structure. H_{AB} is related to the electronic coupling between the electron donor and acceptor in the transition state for the ET reaction. It determines the probability of the reaction occurring when the transition state is achieved. It is maximal when the redox centers are in van der Waals' contact and decreases with distance. The extent of decrease with distance depends on the nature of the intervening medium. The relative efficiencies of ET pathways may be determined according to eq 4,

$$H_{AB} \propto \prod \epsilon_i \tag{4}$$

where ϵ_i is a wave function decay factor for each step in the pathway. The following values have been assigned for these factors (*41*): $\epsilon = 0.6$ for transfer through a covalent bond; $\epsilon = 0.36e^{-1.7(r-2.8)}$ for transfer through a hydrogen bond; and $\epsilon = 0.6e^{-1.7(r-1.4)}$ for a through-space jump. In each case, r is the ET distance. The predicted pathway for ET from TTQ to copper is shown in Figure 7. It is comprised of four sets of steps: one in MADH (inside the TTQ molecule), one through-space jump between the two proteins (Trp108 → $Pro94_{ami}$), and two steps in amicyanin ($Pro94_{ami}$ → $His95_{ami}$ and $His95_{ami}$ → Cu^{2+}). It is clear that it would be inappropriate to consider H_{AB} for this reaction to be related simply to the direct distance between redox centers since the segment of the pathway involving the through-space jump between proteins is much less efficient than the other segments of the pathway. This was shown by the ET analysis between the native MADH and the F97E mutant of amicyanin (*15*), which was best explained by an increase in the interprotein distance at the protein−protein interface which caused the decrease in the ET rate. This residue is present at the MADH−amicyanin interface in the complex. The decrease in H_{AB} correlated more reasonably with an alteration of the single through-space pathway step, rather than applying a uniform β value and assuming an increase in the length of the overall distance between redox centers.

In the studies with αF55A MADH, wild-type amicyanin was used. Thus, the segments of the ET pathway in the amicyanin molecule should be the same for reactions with both native and mutant MADH. The decrease in H_{AB} must be due to a change in the through-space jump from Trp108 to Pro94 of amicyanin or a difference in the distribution of electrons within TTQ. Comparison of the crystal structures of native and αF55A MADH reveals no significant difference in the distance of this through-space jump (3.7 Å in αF55A MADH versus 3.8 Å in native MADH). As discussed earlier, however, movement of the TTQ rings relative to each may occur to achieve the transition state for ET. The observed change in λ suggests that this process may be affected by the mutation. It is possible that the orientation of TTQ in the transition state in native and αF55A MADH is different. This difference need only be subtle. An increase in the distance of the through-space jump of 0.9 Å could account for the observed decrease in H_{AB} using $\epsilon = 0.6e^{-1.7(r-1.4)}$ for a through-space jump.

It should also be noted that, in pathways and distance calculations, the ET from TTQ is taken to occur from the C5′−C6′ edge of Trp108 of TTQ. The initial reduction of TTQ occurs at the C6 position of Trp57 of TTQ. The two Trp rings of TTQ are not in the same plane, with a dihedral angle of about 40°. However, evidence has been obtained previously that indicates that electron delocalization between the two rings does occur (*42*). The extent to which electrons are delocalized throughout the TTQ rings in the transition state for ET will be reflected in the H_{AB} term. Even subtle changes in the orientation of the TTQ rings with respect to each other could affect this property. H_{AB} relates to the coupling between reactants when in the transition state. Therefore, even though the E_m value of MADH is unchanged by the mutation, the electronic distribution in TTQ in the transition state could be affected. If the dihedral angle between TTQ rings influences this distribution, then the effective "starting point" for ET could be different. Such electronic differences in the mutant relative to the native MADH could contribute to the observed differences in H_{AB}, as well as the observed differences in λ.

Conclusion. We have used site-directed mutagenesis to significantly alter the λ value for an interprotein ET reaction. The crystal structures of the native and mutant enzymes are very similar. However, detailed examination reveals subtleties that are consistent with roles of solvent reorganization and protein dynamics in contributing to the λ value for this interprotein ET reaction. Accompanying changes in H_{AB} are also consistent with these hypotheses.

ACKNOWLEDGMENT

The authors thank Yu Tang, Benjie Mangilog, and Yongting Wang for technical assistance.

REFERENCES

1. Davidson, V. L. (2001) *Adv. Protein Chem. 58*, 95−140.
2. Chen, L., Doi, M., Durley, R. C., Chistoserdov, A. Y., Lidstrom, M. E., Davidson, V. L., and Mathews, F. S. (1998) *J. Mol. Biol. 276*, 131−149.
3. McIntire, W. S., Wemmer, D. E., Chistoserdov, A., and Lidstrom, M. E. (1991) *Science 252*, 817−824.

4. Chen, L., Durley, R., Poloks, B. J., Hamada, K., Chen, Z., Mathews, F. S., Davidson, V. L., Satow, Y., Huizinga, E., Vellieux, F. M. D., and Hol, W. G. J. (1992) *Biochemistry 31*, 4959−4964.
5. Chen, L., Durley, R., Mathews, F. S., and Davidson, V. L. (1994) *Science 264*, 86−90.
6. Davidson, V. L., Brooks, H. B., Graichen, M. E., Jones, L. H., and Hyun, Y.-L. (1995) *Methods Enzymol. 258*, 176−190.
7. Bishop, G. R., and Davidson, V. L. (1995) *Biochemistry 34*, 12082−12086.
8. Bishop, G. R., and Davidson, V. L. (1998) *Biochemistry 37*, 11026−11032.
9. Brooks, H. B., and Davidson, V. L. (1994) *Biochemistry 33*, 5696−5701.
10. Brooks, H. B., and Davidson, V. L. (1994) *J. Am. Chem. Soc. 116*, 11202−11202.
11. Marcus, R. A., and Sutin, N. (1985) *Biochim. Biophys. Acta 811*, 265−322.
12. Harris, T. K., Davidson, V. L., Chen, L., Mathews, F. S., and Xia, Z.-X. (1994) *Biochemistry 33*, 12600−12608.
13. Davidson, V. L. (1996) *Biochemistry 35*, 14035−14039.
14. Davidson, V. L. (2000) *Biochemistry 39*, 4924−2928.
15. Davidson, V. L., Jones, L. H., and Zhu, Z. (1998) *Biochemistry 37*, 7371−7377.
16. Ryde, U., Olsson, M. H. M., Roos, B. O., de Kerpel, J. O. A., and Pierloot, K. (2000) *J. Biol. Inorg. Chem. 5*, 565−574.
17. Davidson, V. L., and Jones, L. H. (1996) *Biochemistry 35*, 8120−8125.
18. Zhu, Z., Sun, D., and Davidson, V. L. (2000) *Biochemistry 39*, 11184−11186.
19. Sun, D., and Davidson, V. L. (2001) *Biochemistry 40*, 12285−12291.
20. Davidson, V. L. (1990) *Methods Enzymol. 188*, 241−246.
21. Graichen, M. E., Jones, L. H., Sharma, B. V., van Spanning, R. J., Hosler, J. P., and Davidson, V. L. (1999) *J. Bacteriol. 181*, 4216−4222.
22. Zhu, Z., and Davidson, V. L. (1998) *J. Biol. Chem. 273*, 14254−14260.
23. Chen, L., Mathews, F. S., Davidson, V. L., Tegoni, M., Rivetti, C., and Rossi, G. L. (1993) *Protein Sci. 2*, 147−154.
24. Husain, M., and Davidson, V. L. (1987*) J. Bacteriol. 169*, 1712−1717.
25. Merli, A., Brodersen, D. E., Morini, B., Chen, Z., Durley, R. C. E., Mathews, F. S., Davidson, V. L., and Rossi, G. L. (1996) *J. Biol. Chem. 271*, 9177−9180.
26. Otwinowski, Z. and Minor, W. (1997) *Methods Enzymol. 276*, 307−326.
27. Navaza, J. (1994) *Acta Crystallogr., Sect. A 50*, 157−163.
28. Allen, F. H., and Kennard, O. (1993) *Chem. Des. Autom. News 8*, 1−31.
29. Brünger, A. T., Adams, P. D., Clore, G. M., DeLano, W. L., Gros, P., Grosse-Kunstleve, R. W., Jiang, J. S., Kuszewski, J., Nilges, M., Pannu, N. S., Read, R. J., Rice, L. M., Simonson, T., and Warren, G. L. (1998) *Acta Crystallogr., Sect. D 54*, 905−921.
30. Kleywegt, G. J., and Brünger, A. T. (1996) *Structure 4*, 897−904.
31. Jiang, J.-S., and Brünger, A. T. (1994) *J. Mol. Biol. 243*, 100−115.
32. Roussel, A., and Cambillau, C. (1991) in *Silicon Graphics Geometry Partners Directory 86*, Silicon Graphics, Mountain View, CA.
33. Ramachandran, G. N., and Sasisekharan, V. (1968) *Adv. Protein Chem. 23*, 283−438.
34. Laskowski, R. A., MacArthur, M. W., Moss, D. S., and Thornton, J. M. (1993) *J. Appl. Crystallogr. 26*, 283−291.
35. Labesse, G., Ferrari, D., Chen, Z.-W., Rossi, G. L., Kuusk, V., McIntire, W. S., and Mathews, F. S. (1998) *J. Biol. Chem. 273*, 25703−25712.
36. Wang, Y., Sun, D., and Davidson, V. L. (2002) *J. Biol. Chem. 277*, 4119−4122.
37. Sun, D., and Davidson, V. L. (2002) *FEBS Lett. 517*, 172−174.
38. Hyun, Y.-L., Zhu, Z., and Davidson, V. L. (1999) *J. Biol. Chem. 274*, 29081−29086.
39. Chistoserdov, A. Y. (2001) *Microbiology 147*, 2195−2202.
40. Hyun, Y.-L., and Davidson, V. L. (1995) *Biochemistry 34*, 816−823.
41. Regan, J. J., Risser, S. M., Beratan, D. N., and Onuchic, J. N. (1993) *J. Chem. Phys. 97*, 13083−13088.
42. Singh, V., Zhu, Z., Davidson, V. L., and McCracken, J. L. (2000) *J. Am. Chem. Soc. 122*, 931−938.

BI026654X